PHYSICAL REVIEW B, VOLUME 63, 161308(R)

Homogeneous broadening and excitation-induced dephasing of intersubband transitions in a quasi-two-dimensional electron gas

Robert A. Kaindl, Klaus Reimann, Michael Woerner, and Thomas Elsaesser
Max-Born-Institut für Nichtlineare Optik und Kurzzeitspektroskopie, D-12489 Berlin, Germany

R. Hey and K. H. Ploog
Paul-Drude-Institut für Festkörperelektronik, D-10117 Berlin, Germany
(Received 13 February 2001; published 6 April 2001)

The irreversible decay of coherent intersubband polarizations in *n*-type modulation-doped $GaAs/Al_xGa_{1-x}As$ quantum wells is studied by femtosecond time-integrated and time-resolved four-wave mixing. We provide the first direct evidence for predominant homogeneous broadening of intersubband resonances by intraband electron-electron scattering. Even at a low electron concentration of 5×10^{10} cm^{-2} the dephasing time $T_2=320$ fs accounts fully for the 4 meV intersubband linewidth. For 6×10^{11} electrons/cm^2 and strong excitation, athermal electron distributions show enhanced dephasing rates.

DOI: 10.1103/PhysRevB.63.161308 PACS number(s): 78.47.+p, 73.21.−b

Intersubband (IS) transitions of quantum-confined carriers are relevant both for nonequilibrium carrier dynamics and for optical properties of low-dimensional systems.[1] In quasi-two-dimensional semiconductors, optical IS transitions are strongly influenced by Coulomb interaction among the carriers and thus provide a sensitive probe of microscopic interactions and of the resulting ultrafast dynamics. Moreover, IS transitions play an important role for devices like the quantum cascade laser.[2]

The properties of optical IS transitions, in particular the spectral position and line shape of the stationary IS absorption spectra of electrons, have been the subject of numerous theoretical and experimental studies. In general, there are three major effects of Coulomb interaction on the lineshape: First, depolarization in a dense 2D electron plasma leads to a blueshift of the absorption band together with a line narrowing for a nonparabolic in-plane dispersion.[3] Second, direct and exchange Coulomb interactions result in a spectral redistribution of oscillator strength and a reshaping of the absorption spectrum, thereby partly compensating the depolarization shift.[4–7] Third, Coulomb scattering among electrons is a dephasing process of the coherent macroscopic IS polarization, contributing to the homogeneous broadening of IS absorption lines.[8,9]

The first two effects of Coulomb interaction have been studied in quite some detail by observing the changes of IS absorption lines in heterostructures or quantum wells (QWs) as a function of equilibrium parameters such as temperature or electron concentration. In contrast, experimental information about the amount of homogeneous broadening and the influence of Coulomb scattering on IS dephasing remains scarce. To grasp the IS polarization dynamics, nonlinear optical techniques, e.g., four-wave mixing, are required. So far, subpicosecond IS dephasing has been studied only for electrons in strongly disordered $Ga_yIn_{1-y}As/Al_xIn_{1-x}As$ QWs exciting a small fraction of the electrons present by doping.[10] The strong inhomogeneous broadening of the IS transition in such samples leads to a fast photon-echolike polarization decay, hindering a study of dephasing rates for different nonequilibrium electron distributions. Moreover, the much discussed dephasing by Coulomb scattering at low electron concentrations has remained unresolved.

In this paper, we investigate IS dephasing in high quality $GaAs/Al_xGa_{1-x}As$ QWs with negligible disorder-induced inhomogeneous broadening, for electron concentrations as low as 5×10^{10} cm^{-2}, and as a function of excitation intensity. Ultrafast time-integrated (TI) and time-resolved (TR) detection of four-wave-mixing (FWM) transients in the mid-infrared demonstrates for the first time that irreversible dephasing processes on a time scale of several hundreds of femtoseconds represent the predominant broadening mechanism at such low carrier concentrations, resulting in a homogeneously broadened IS absorption line of less than 4 meV width. Experiments give evidence of IS phase relaxation dominated by intrasubband Coulomb scattering. For an electron concentration of 6×10^{11} cm^{-2}, the experiments as a function of excitation density demonstrate that an increase in phase space available for scattering results in faster IS dephasing.

We investigated two QW samples with different electron concentrations: sample *A* consists of 51 GaAs QWs of 10-nm width, separated by 20-nm-thick $Al_{0.35}Ga_{0.65}As$ barriers, the centers of which are *n*-type δ-doped with Si. This results in an electron concentration $n_s=5\times10^{10}$ cm^{-2} per QW. Sample *B* is doped to a higher electron concentration $n_s=6\times10^{11}$ cm^{-2}, containing 6 wells of 9 nm width. The two samples show comparable overall absorbances $A_{IS}\approx0.8$ (sample *A*) and $A_{IS}\approx0.6$ (sample *B*). Both samples were processed into small prisms to achieve a strong coupling between the *p*-polarized light field entering through the front facet of the prism and the IS transition dipole which is oriented perpendicular to the QW layers. The $n=1$ to $n=2$ IS absorption spectra are shown in the insets of Fig. 1, demonstrating very small IS line widths of $\Delta E_{IS}=3.7$ meV (FWHM) for sample *A*, and $\Delta E_{IS}=6.3$ meV for sample *B*. In the femtosecond experiments, the $n=1$ to $n=2$ IS transition was excited resonantly by 130-fs mid-infrared pulses ($\lambda=9-15$ μm), which were generated by nonlinear frequency conversion of amplified pulses from a Ti:sapphire laser.[12]

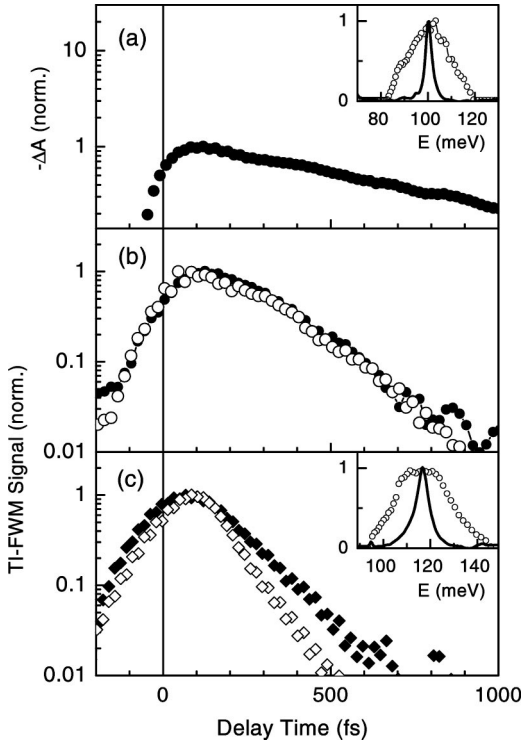

FIG. 1. (a) Bleaching dynamics of IS absorption in $GaAs/Al_xGa_{1-x}As$ quantum wells after resonant femtosecond excitation (electron concentration $n_s = 5\times10^{10}$ cm^{-2}, sample *A*). The spectrally integrated absorption change $\Delta A = -\int d\omega \ln[T(\omega)/T_0(\omega)]$ (symbols) is plotted versus pump-probe time delay. It is proportional to the $n=2$ subband population and decays exponentially with $T_1 = 550$ fs. (b) Time-integrated (TI) FWM intensity in the diffracted direction $2\mathbf{k}_2 - \mathbf{k}_1$ for pulse intensities $I_0 = 0.7$ MW/cm^2 (solid circles) and 6 I_0 (open circles) in sample *A* as a function of time delay $\Delta t_{12} = t_2 - t_1$ between the incident pulses. (c) Same as (b), but for higher $n_s = 6\times10^{11}$ cm^{-2} (sample *B*). Insets: Corresponding normalized IS absorption profiles (lines) and pulse spectra (circles).

The spectra of the mid-infrared pulses are also shown in Fig. 1. The measurements were performed at a lattice temperature of $T_L = 15$ K.

The lifetime T_1 of electrons in the $n=2$ subband was determined by pump-probe measurements. The nonlinear change of IS absorption induced by the pump pulse (peak intensity $I_0 = 0.7$ MW/cm^2) was monitored by weak delayed probe pulses.[13] In Fig. 1(a), the spectrally integrated absorption change $\Delta A = -\int d\omega \ln[T(\omega)/T_0(\omega)]$ of sample *A* is plotted as a function of the delay time between pump and probe (T, T_0: sample transmission with and without excitation). The strong nonlinear decrease of IS absorption decays by relaxation of $n=2$ electrons back to the $n=1$ subband via the emission of longitudinal optical phonons.[14] Both samples show a time constant of $T_1 = 550$ fs.

Coherent IS polarizations were studied in degenerate four-wave-mixing (FWM) experiments. Two mid-infrared pulses with wavevectors $\mathbf{k}_1$ and $\mathbf{k}_2$ generate a transient grating in the sample from which third-order signals are self-diffracted into the directions $2\mathbf{k}_2 - \mathbf{k}_1$ and $2\mathbf{k}_1 - \mathbf{k}_2$. The signal in the direction of $2\mathbf{k}_2 - \mathbf{k}_1$ was detected either by a time-integrating HgCdTe detector or by time-resolved upconversion. For TR detection, the sum frequency of the diffracted signal and a synchronized reference pulse (width 100 fs, wavelength 1.3 μm) generated in a 1-mm-thick GaSe crystal was recorded as a function of time delay between signal and reference pulses (for details, see Ref. 12).

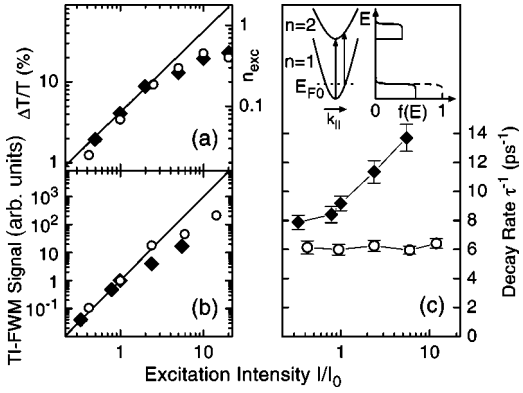

FIG. 2. Results for various excitation intensities for electron concentrations of 5×10^{10} cm^{-2} (open circles) and 6×10^{11} cm^{-2} (solid diamonds): (a) Amplitudes of induced bleaching $\Delta T/T_0$ in the pump-probe signals (symbols) compared with a linear response (solid line). The fraction of excited electrons (right ordinate scale) was estimated by comparison with model calculations. (b) Amplitude of the TI-FWM signal (symbols) compared to a cubic intensity dependence $(I/I_0)^3$ (solid line). (c) Decay rate τ^{-1} of the TI-FWM signals as a function of excitation intensity. Inset: schematic subband dispersion, and distribution functions before (dashed line) and directly after (solid line) excitation.

In Figs. 1(b) and 1(c), TI-FWM signals are shown for both samples and for low and high excitation intensity I/I_0. The spectrally integrated signals are plotted as a function of time delay Δt_{12} between the two pulses generating the transient grating. In all cases, the signals rise within the time resolution of the experiment, exhibit a delayed peak at ≈ 100 fs, and subsequently decay on a time scale of several hundreds of femtoseconds, reflecting the decay of the macroscopic IS polarization $P^{(3)}$. At low excitation intensities [solid symbols, Figs. 1(b) and 1(c)] one finds a decay time of $\tau = 160 \pm 15$ fs for sample *A* and $\tau = 130 \pm 10$ fs for sample *B*, both significantly faster than the population decay. For stronger excitation (open symbols) the dynamics of sample *A* remains unchanged, whereas sample *B* shows a substantially faster decay.

Figures 2(a) and 2(b) show the induced pump-probe amplitudes and the TI-FWM signal intensity versus I/I_0. The saturation of the pump-probe signals allows to estimate the fraction n_{exc} of excited $n=1$ carriers [Fig. 2(a)]. For low intensities, the diffracted FWM signal shows a cubic dependence on I/I_0 [Fig. 2(b)], as expected for a third-order nonlinear process. The diffracted signal begins to saturate when a substantial fraction of $n=1$ electrons is excited into the $n=2$ subband. The corresponding decay rates τ^{-1} of the TI-FWM signals are plotted in Fig. 2(c). For low electron concentration (sample *A*, circles), the decay rate of the TI-FWM signal is practically independent of I/I_0. In contrast, a significant increase of the decay rate with excitation intensity is

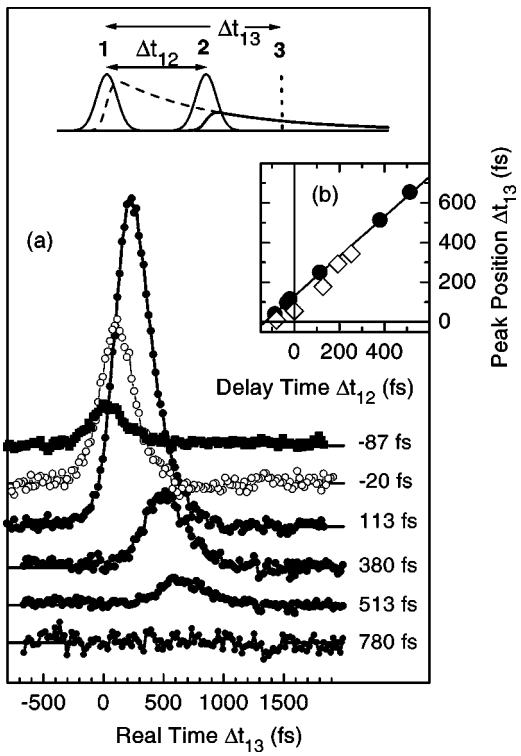

FIG. 3. (a) Time-resolved FWM transients for sample *A* detected by sum-frequency mixing of the mid-infrared FWM transients with near-infrared pulses ($\lambda = 1.3\ \mu$m) in GaSe. Signals are shown as a function of real time delay Δt_{13} between the near-infrared pulse 3 and the mid-infrared pulse 1, at various fixed delays Δt_{12}. Inset: pulse sequence. (b) Peak positions of the transients for different Δt_{12} (filled circles), compared to a linear dependence $\Delta t_{13} = \Delta t_{12} + 130$ fs (solid line). Diamonds: corresponding results for sample *B*.

observed in the case of higher electron concentration (sample *B*, diamonds).

To unambiguously distinguish between homogeneous and inhomogeneous broadening we have performed the first TR-FWM study of IS polarizations. In Fig. 3(a), TR-FWM signals diffracted from sample *A* in $2\mathbf{k}_2 - \mathbf{k}_1$ direction are plotted versus the real time delay Δt_{13} between pulse 1 and the reference pulse 3 (inset) for different time delays Δt_{12}. With increasing Δt_{12}, the maximum of the TR-FWM signal shifts monotonously to later times and the peak position as a function of Δt_{12} [Fig. 3(b), circles] reveals a linear dependence $\Delta t_{13} = m\,\Delta t_{12} + 130$ fs (solid line) with the slope $m = 1$. A similar behavior is found for sample *B* [Fig. 3(b), diamonds]. In both cases, the signal integrated over Δt_{13} reproduces the TI-FWM signal as a function of Δt_{12}.

In the following, we first discuss the dynamics of the macroscopic IS polarization and the resulting broadening of the IS absorption line. In general, the IS dephasing dynamics is influenced by (i) the destructive interference between polarization components with different transition frequencies in an inhomogeneously broadened ensemble, each evolving differently in time, and (ii) the *irreversible* phase loss of the IS polarization due to scattering processes, resulting in a homogeneous broadening. The temporal structure of TR-FWM signals gives direct information about the relative strength of these two contributions, and about the presence of many-body effects caused by the Coulomb interaction among the electrons, directly affecting the polarization dynamics. The data in Fig. 3 display a linear shift of the maximum of the TR-FWM signals with increasing time delay Δt_{12} and a slope $m = 1$ for both samples. This behavior is indicative of a free induction decay of the macroscopic polarization and gives direct evidence for a predominant homogeneous broadening of the IS resonance in both samples.[15] Based on this finding, one derives an IS dephasing time $T_2 = 2\tau = 320 \pm 30$ fs from the decay of the TI-FWM signal of sample A at $T_L = 15$ K [Fig. 1(c)]. This translates into a homogeneous linewidth of 4.0 ± 0.4 meV, accounting very well for the linewidth of the steady state IS absorption of 3.7 meV [Fig. 1(a)]. Such excellent agreement is also found for higher lattice temperatures and demonstrates that inhomogeneous line broadening due to static disorder, which would lead to fluctuations of the IS transition energy, or from subband nonparabolicity plays a minor role. Depolarization and excitonic effects are almost absent at the low electron concentration of $n_s = 5 \times 10^{10}\ \mathrm{cm}^{-2}$.[3–7]

An analysis for higher electron concentration (sample *B*) demonstrates that the IS absorption line (width 6.3 meV at $T_L = 15$ K) is homogeneously broadened also in this case. A single-particle picture of IS absorption predicts a small inhomogeneous broadening of 1.2 meV due to different dispersions of the two subbands. However, many-body effects result in a coupling of transitions at different energies, reducing this inhomogeneous broadening substantially.[4] The influence of such effects on the FWM signals are expected to be negligible.[11]

We now consider the microscopic mechanisms underlying IS dephasing. For resonant IS excitation, electrons in both the $n = 1$ and $n = 2$ subband transiently populate states well below the LO phonon energy and thus intraband LO phonon emission is suppressed. The rates of intraband LO phonon absorption at such low temperatures ($T_L = 15$ K) and of intraband acoustic phonon scattering are orders of magnitude too small to account for the observed dephasing dynamics. The irreversible loss of intersubband phase measured by the rate T_2^{-1} can occur due to population relaxation with a contribution of $(2T_1)^{-1}$ and due to ''pure'' dephasing caused by phase-breaking scattering processes within each subband with a rate $(T_2^*)^{-1}$. The experimentally determined $T_1 = 550$ fs give a rate $(2T_1)^{-1} = 0.9\ \mathrm{ps}^{-1}$ [Fig. 1(a)], clearly smaller than the dephasing rates of $3-4\ \mathrm{ps}^{-1}$. Thus intrasubband Coulomb scattering among electrons dominates the irreversible dephasing of coherent intersubband polarizations, even in the case of very low plasma densities studied here.[10]

Our intensity-dependent measurements, in which the total electron concentration remains constant, provide new information on IS dephasing by Coulomb scattering for strong nonequilibrium excitation. With increasing excitation intensity, a bigger fraction of electrons is excited to the $n = 2$ subband, resulting in a athermal electron distribution with strong population of both the $n = 1$ and $n = 2$ subband.

At intensities of $I=6I_0$ about 30% of the $n=1$ electrons are excited into the $n=2$ subband [Fig. 2(a)]. For the higher electron concentration $n_s=6\times10^{11}$ cm^{-2} (sample *B*)—corresponding to an initial Fermi energy of $E_{F0}=21$ meV—the phase space available for electron-electron scattering is significantly increased due to the energy and momentum independent depletion of carriers through the broadband femtosecond excitation [cf. Fig. 2(c)]. This results in a strong increase of dephasing rates [Fig. 2(c), diamonds]. For sample *A*, however, the Fermi energy of 1.8 meV is too low to allow for a significant modification of the available phase space and consequently the dephasing rates are independent of the excitation intensity [circles in Fig. 2(c)].

So far, a microscopic theory of IS dephasing by electron-electron scattering has not been developed. Nevertheless, electron-electron interactions in QWs have been analyzed in various approximations, giving electron scattering times similar to the dephasing times T_2 found here. The broadening of an IS resonance at about 130 meV by electron-electron scattering in a 8-nm-wide GaAs/$Al_{0.35}Ga_{0.65}$As QW was calculated taking into account the structure of the two-dimensional plasma excitations in a full dynamically screened RPA approach.[9] The resulting scattering rates depend strongly on the energy position of a ''hole,'' i.e., unoccupied electron state, below the Fermi level in the lower subband, and vary from 0 to 6 ps^{-1}. This gives an average rate of ≈3 ps^{-1}, in good agreement with the dephasing rate found in our experiment. Similar scattering rates were found for electrons close to the subband minima of GaAs/$Al_{0.35}Ga_{0.65}$As QWs at low temperatures using a dynamic RPA approach.[8] In these calculations, however, a much smaller IS energy spacing of ≈20 meV was considered.[16]

In summary, electron-electron scattering results in subpicosecond IS dephasing, even at electron concentrations as low as 5×10^{10} cm^{-2}. The dephasing rates increase strongly with the amount of phase space available for scattering as is evident from femtosecond four-wave-mixing experiments with strong IS excitation. Time-resolved detection of the FWM signals demonstrate unambiguously that the narrow IS absorption lines of high quality GaAs/Al_xGa_{1-x}As quantum wells are predominantly homogeneously broadened.

[1] For a review see, T. Elsaesser and M. Woerner, Phys. Rep. **321**, 253 (1999).
[2] J. Faist *et al.*, Science **264**, 553 (1994).
[3] S. Graf *et al.*, Phys. Rev. Lett. **84**, 2686 (2000).
[4] M. Zaluzny, Phys. Rev. B **43**, 4511 (1991); **49**, 2923 (1994).
[5] M. S.-C. Luo *et al.*, Phys. Rev. B **48**, 11 086 (1993).
[6] D. E. Nikonov *et al.*, Phys. Rev. Lett. **79**, 4633 (1997).
[7] S. Tsujino *et al.*, Phys. Rev. B **62**, 1560 (2000).
[8] S.-C. Lee and I. Galbraith, Phys. Rev. B **55**, 16 025 (1997); **59**, 15 796 (1999).
[9] P. v. Allmen, Phys. Rev. B **46**, 13 345 (1992); **46**, 13 351 (1992).
[10] R. A. Kaindl *et al.*, Phys. Rev. Lett. **80**, 3575 (1998).
[11] B. Nottelmann, V. M. Axt, and T. Kuhn, Physica B **272**, 234 (1999).
[12] R. A. Kaindl *et al.*, J. Opt. Soc. Am. B **17**, 2086 (2000).
[13] The intensity is determined from the focus diameter, the pulse duration, and the pulse energy.
[14] R. Ferreira and G. Bastard, Phys. Rev. B **40**, 1074 (1989).
[15] In contrast, signals from inhomogeneously broadened transitions would show a photon echo behavior with a slope $m=2$.
[16] For such small IS spacing, electron-electron scattering even contributes to IS population relaxation, see, e.g., M. Hartig *et al.*, Phys. Rev. Lett. **80**, 1940 (1998).